JACS
JOURNAL OF THE AMERICAN CHEMICAL SOCIETY

Article

pubs.acs.org/JACS

Mesoscale Modulation of Supramolecular Ureidopyrimidinone-Based Poly(ethylene glycol) Transient Networks in Water

Roxanne E. Kieltyka,[†,‡] A. C. H. Pape,[†,‡] Lorenzo Albertazzi,[†,‡] Yoko Nakano,[†,‡,§] Maartje M. C. Bastings,[†,‡] Ilja K. Voets,[†,§] Patricia Y. W. Dankers,[†,‡] and E. W. Meijer*[,†,‡,§]

[†]Institute for Complex Molecular Systems, [‡]Laboratory of Chemical Biology, and [§]Laboratory of Macromolecular Organic Chemistry, Eindhoven University of Technology, P.O. Box 513, 5600 MB Eindhoven, The Netherlands

Supporting Information

ABSTRACT: In natural systems, highly synergistic non-covalent interactions among biomolecular components exert mesoscopic control over hierarchical assemblies. We herein present a multicomponent self-assembly strategy to tune hierarchical supramolecular polymer architectures in water using highly affine and directional ureidopyrimidinone-poly(ethylene glycol)s (UPy-PEG). Using scattering methods and oscillatory rheology, we observe the structural and mechanical regulation of entangled monofunctional UPy-PEG fibrils by cross-linking bifunctional UPy-PEG fibrils. This supramolecular mixing approach opens the door to a range of subtly distinct materials for chemical and biological applications.

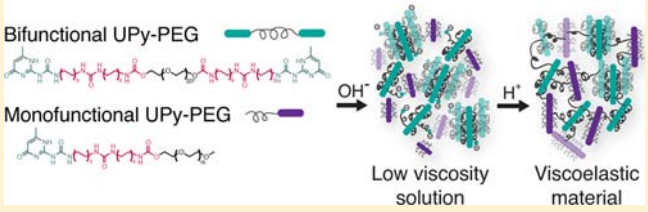

INTRODUCTION

Control over the mesoscale in biomolecule assemblies is highly important for basic cellular function and response to external stimuli. One specific example of such control is the direct cross-linking of macromolecular F-actin chains, composed of G-actin monomers, by actin-binding proteins, such as α-actinin.[1,2] The non-covalent interaction of these proteins promotes their hierarchical organization into kinetically trapped gel-like materials in the cytosol. Intriguingly, assemblies of actin filaments have been observed at exceedingly low molar ratios of cross-linker protein, such as 1:90 in α-actinin/G-actin.[1] This natural strategy would be highly attractive to tune aqueous supramolecular polymer architectures[3−8] at the mesoscale.

Supramolecular materials based on one-dimensional self-assembled fibrils have been described for several systems, such as low-molecular-weight compounds,[9−11] peptides,[12−17] and supramolecular polymers.[18] The common mode of transient network formation in these systems is through entanglement of supramolecular fibrils of one component above a critical concentration, resulting in remarkable viscoelastic properties. An alternate method to obtain such materials is through a multicomponent approach, where more than one component is used.[19,20] For two-component systems, this area can be further subdivided into three general gel classes:[19] those that only form gels when both components are added,[21] those that independently form gels and the components mix[22] or self-sort[23] once combined, and those whose physical properties can be modulated by non-gelating additives.[24] Despite extensive exploration into the self-assembly characteristics of two-component materials in organic media, far less is known regarding the hierarchical modulation of supramolecular assemblies in aqueous media. Inspired by the hierarchical organization of actin filaments by proteins, we sought to determine if similar principles could be applied to artificial supramolecular systems in water.

We recently reported the preparation of a ureidopyrimidinone-poly(ethylene glycol)-based bifunctional supramolecular polymer (UPy-PEG **1**, Figure 1) that has the capacity to self-assemble into fibrillar aggregates that can directly cross-link one another by virtue of their complementary non-covalent interactions in water.[25] These UPy-PEG supramolecular polymers are composed of directionally hydrogen-bonding UPy and urea moieties within a hydrophobic spacer (C6−U−C12) to shield them from the aqueous environment. The hydrophobic segments are opposite a poly(ethylene glycol) spacer (molecular weight 5−20 kDa) to guide phase segregation into hierarchical supramolecular motifs. Upon increasing the concentration, self-healing aqueous supra-

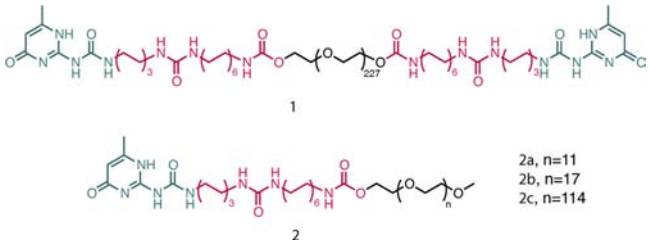

Figure 1. Chemical structures of UPy-PEG supramolecules: bifunctional **1** and monofunctional **2a−c**.

Received: April 15, 2013
Revised: July 4, 2013
Published: July 7, 2013

   dx.doi.org/10.1021/ja403745w | J. Am. Chem. Soc. 2013, 135, 11159−11164

molecular transient networks were obtained by a thermal protocol and applied for growth factor delivery applications.

In this work, we introduce monofunctional UPy-PEG **2** (Figure 1) that self-assembles into a weak 3D network in water as a function of its PEG chain length. By exploiting bifunctional UPy-PEG **1** as a supramolecular polymer cross-linker, we dramatically alter the mechanical properties of the resultant aqueous materials upon mixing with **2** at various ratios. Strikingly, with small amounts of **1** added to **2a** and **2b**, a strong synergistic effect is observed, yielding strong and stable hydrogels outperforming both individual components. However, when mixed with **2c** bearing a longer PEG chain (~5000 Da), the synergistic effect disappears. We explore the mode of interaction of this synergistic effect of these two *a priori* gel-forming components **1** and **2a** or **2b** in the aqueous material mixture.

RESULTS AND DISCUSSION

Design and Synthesis. Non-covalent synthesis of supramolecular materials in the aqueous environment requires careful consideration of the molecular design of all components to yield a stable, yet dynamic material. For this purpose, the high-fidelity, four-point hydrogen bonding UPy motif was employed. Shielding of the UPy units from water while increasing their proximity to one another was accomplished through the use of hydrophobic alkyl chains linked by a urea moiety (C6−U−C12). To increase solubility and to guide microphase separation into fibrillar morphologies, monomethoxylated poly(ethylene glycol)s were used to decorate the hydrophobic hydrogen-bonding fragments (Figure 1). We designed short monofunctional units **2a,b** with 517 and 781 Da poly(ethylene glycols), respectively. Poly(ethylene glycol) with molecular weight of 10 000 Da was used for the bifunctional UPy cross-linker **1**. As a reference, we designed monofunctional **2c** bearing a 5000 Da poly(ethylene glycol) chain, being roughly half of **1** in molecular weight.

The synthesis of **2a,b** is given in Scheme 1 and starts with the CDI activation of **3a,b** and reaction with Cbz-protected dodecyl diamine, providing **4a,b** in good yields (70−88%). Subsequent deprotection of the Cbz protecting group using Et_3SiH/Pd/C, followed by reaction of the free amine with UPy-hexyl-isocyanate, resulted in monofunctional UPy-PEG amphiphiles **2a,b** (yields 42−61%). Efficient one-pot syntheses and facile purification by C18 column chromatography of **2a,b** permitted rapid access and scalability. Polymer **2c** was conveniently synthesized by activation of the poly(ethylene glycol) monomethyl ether with 1,1-carbonyldiimidazole and subsequent reaction with an excess of 1,12-diaminododecane to give the amine-terminated PEG in moderate yields (59%). The latter was reacted with UPy-hexyl-isocyanate and purified by precipitation, resulting in amphiphile **2c** (yield 58%).

Scheme 1. Synthetic Protocol To Obtain Monofunctional UPy-PEG 2a,b[a]

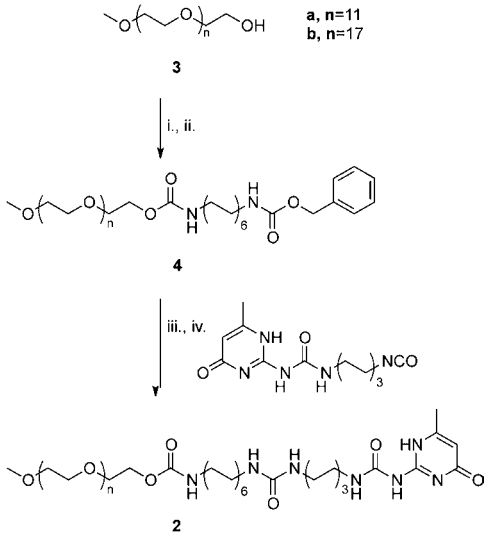

[a]Reagents: (i) CDI, $CHCl_3$; (ii) $CbzNHC_{12}NH_2$, DIPEA, reflux, $CHCl_3$; (iii) Et_3SiH, Pd/C, MeOH; (iv) $UPyC_6NCO$, $CHCl_3$.

Hierarchical Self-Assembly. In order to build two-component supramolecular materials, insight into the self-assembly characteristics of each component *a priori* is required. All UPy-PEG molecules (**1** and **2**) were first dissolved through the addition of base (0.1 M NaOH) and self-assembled into their respective morphologies using acid (0.1 M HCl) at 20 °C. Two distinct states of the UPy moiety were observed in FTIR measurements when samples of **2b** were measured in D_2O, D_2O with 0.1 M NaOH, and D_2O with 0.1 M NaOH and 0.1 M HCl (Figure 2). IR spectra acquired for **2b** were similar to those previously obtained for bifunctional molecule **1** (see Supporting Information).[26] The IR spectra in the C═O stretching region show a pattern with three peaks at around 1668, 1602, and 1535 cm^{-1} in the acidic (0.1 M HCl, pH ~3) or neutral conditions. In contrast, four peaks at around 1685, 1632, 1598, and 1535 cm^{-1} are observed in basic conditions (0.1 M NaOH, pH ~12). The IR data are consistent with deprotonation of the UPy motif into the enolate anion at high pH followed by protonation upon lowering the pH. These data were further supported by zeta potential measurements, where negative values were found upon dissolution using basic conditions (ZP = −42.8 mV) suggestive of enolate formation on the UPy moiety, with a return to more positive values (ZP = −12.7 mV) upon acidification. The precise zeta potential values varied accordingly with the molar concentration of acid or base in the stock solution.

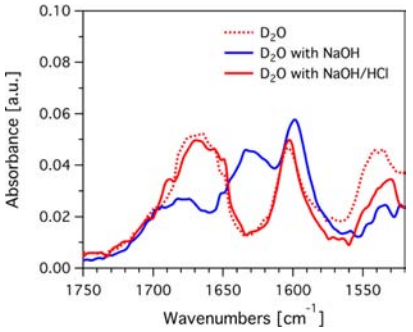

Figure 2. Infrared spectra recorded in amide I (C═O stretching) and amide II (coupling of N−H bending and C−N stretching) regions of 1.0 wt% solution of **2b** and **1** in D_2O (dotted line), under basic (0.1 M NaOH in D_2O, pH ~12) (solid red line) and acidic (0.1 M NaOH + 0.1 M HCl in D_2O, pH ~3) (solid blue line) conditions.

Complete dissolution to the molecular level of **1** and **2** at high pH was not achieved—and not required for further applications—as polydisperse fibrillar species of **2b** were observed by small-angle X-ray scattering (SAXS), confocal microscopy, and atomic force microscopy (AFM) experiments.

dx.doi.org/10.1021/ja403745w | J. Am. Chem. Soc. 2013, 135, 11159−11164

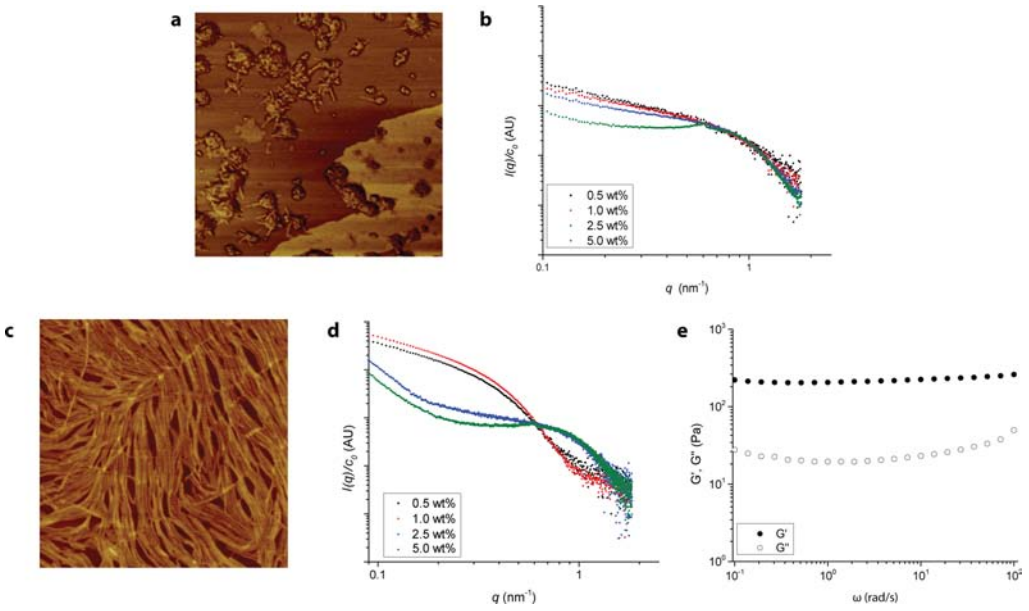

Figure 3. Self-assembly of **2b**. Under basic conditions (0.1 M NaOH, pH ∼12): (a) Representative atomic force micrograph (phase) drop-cast on mica from a 0.002 wt% solution. Scale of image is 3 × 3 μm. (b) Small-angle X-ray scattering profiles, $I(q)$ in arbitrary units, as a function of the magnitude of the scattering vector, q in nm^{-1}, divided by concentration for 0.5, 1.0, 2.5, and 5.0 wt% solutions. After acidification (0.1 M NaOH + 0.1 M HCl, pH ∼3): (c) AFM (height) image drop-cast on mica from a 0.002 wt% solution. Scale of image is 3 × 3 μm. (d) SAXS profiles (0.5, 1.0, 2.5, and 5.0 wt%) *vide supra*. (e) Frequency sweep of a 5.0 wt% sample (1% strain, 0.1−100 rad/s).

In AFM experiments (Figure 3a) in the dry state, truncated fibrils were observed under basic conditions (0.1 M NaOH, pH ∼12). Upon acidification (0.1 M HCl, pH ∼3) of the basic solution long, fibrillar objects of molecules **2b** were found ∼10 nm in width and micrometers in length by atomic force microscopy (0.002 wt%, Figure 3c). The features of the fibrillar constructs of **2a** are similar to those of **2b** (see Supporting Information). SAXS experiments further support the presence of rod-like structures under all conditions (Figure 3b,d). Under acidic conditions up to 1.0 wt% fibers with a cross-sectional radius of gyration (R_{cgs}) of 4.5 nm are observed (Figure 3d and Supporting Information). An increase in the concentration of **2b** up to 5.0 wt% results in a transition to an interacting network of self-assembled fibrils as evidenced by the marked decrease in slope at intermediate q values (0.4−0.5 nm^{-1}) under acidic conditions. At the highest weight percentage of **2b** a viscoelastic response was obtained by oscillatory rheology on the order of 10^2 Pa (Figure 3e).

Confocal microscopy experiments further support the formation of an interacting network of fibrils. Micrometer-size aggregates of **2b**, polydisperse in size, were found upon using a solvatochromic dye, Nile red, as a probe of hydrophobic environment (see Supporting Information). The width of these fibers is below the resolution of the instrument, on the order of a few hundreds of nanometers. Aggregates of **2b** under basic conditions increased in number concomitantly with concentration (0.01−5.0 wt%) until a homogeneous fluorescent signal was observed at the highest weight percentage. Proportionate with the concentration of **2b**, fluorescence spectra showed significant hypsochromic shifts of the Nile red peak maxima ($\Delta\lambda$ = 8−18 nm) relative to that of the free dye in water (660 nm). Confocal microscopy of **2b** in solution after the addition of acid showed a high density of flexible, micrometer long fibers at the lowest weight percentage (0.01 wt%) and a phase-separated mixture at the highest value (5 wt%) (see Supporting Information movies). Fluorescence spectra showed even stronger hypsochromic shifts ($\Delta\lambda$ = 15−20 nm) reflecting the increased hydrophobicity arising from fibril formation in more acidic (pH ∼3) conditions.

Based on these studies, the monofunctional UPy-PEG molecules **2a,b** self-assemble into one-dimensional aggregates. Compounds **2b**, and by extrapolation **2a** (*vide infra*), can form weak 3D networks through entanglement of their supramolecular polymer chains.

Aqueous Materials Composed of 1 and 2a,b. In order to modulate the hierarchical interaction of the monofunctional UPy-PEG supramolecular polymer fibers of **2a,b**, both molecules **1** and **2a,b** were mixed in the solid state prior to dissolution. Within 90 min after acidification, relatively rigid, kinetically trapped viscoelastic materials were formed for the combinations of **1** with either **2a** or **2b** (Figures 4 and 5). Representative frequency sweep curves for these mixtures are given in Figure 6a,b. Remarkably, titration of small amounts of cross-linker **1**, as low as 0.1 wt%, to **2a** or **2b** resulted in

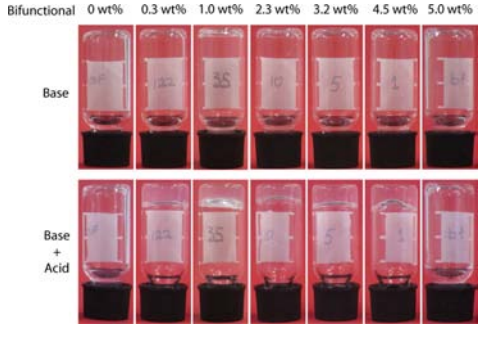

Figure 4. Mixing supramolecules **1** and **2b**, on a total of ∼5 wt%, yields a low viscosity liquid under basic (0.1 M NaOH, pH ∼12) conditions (top) and subsequently, viscoelastic materials of varied elastic modulus after 90 min after acidification (0.1 M HCl, pH ∼3) (bottom).

dx.doi.org/10.1021/ja403745w | J. Am. Chem. Soc. 2013, 135, 11159−11164

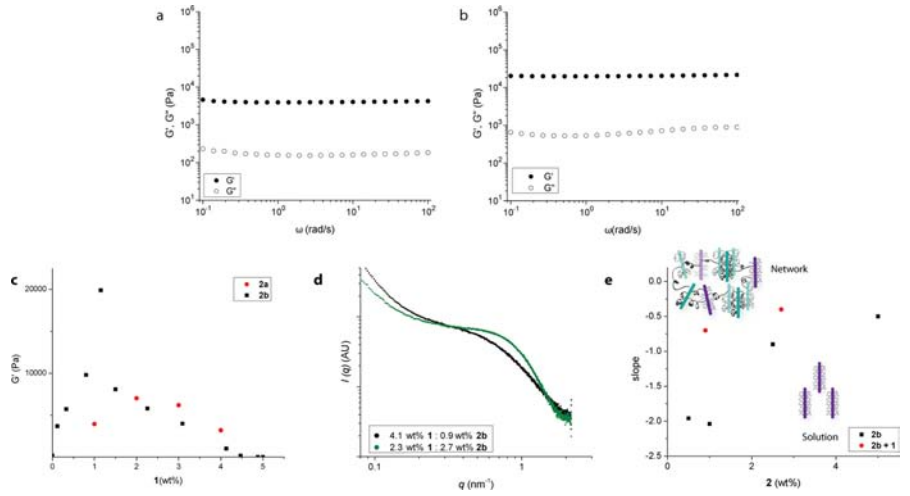

Figure 5. Mixed supramolecular materials composed of **1** and **2a,b** after acidification (pH ~3). Oscillatory rheology measurements, frequency sweep measurements (1% strain, 0.1−100 rad/s), and representative profiles of (a) **1**, 1 wt% and **2a**, 4 wt%; (b) 1, 1.1 wt% and **2b**, 3.9 wt%. (c) Comparison of the plateau modulus at 1 rad/s as a function of increasing weight percentage of **1** with **2a,b** from frequency sweep measurements. Small angle X-ray measurements: (d) scattering profiles of supramolecular hydrogels of 4.1 wt% **1** and 0.9 wt% **2b** (black circles) and 2.3 wt% **1** and 2.7 wt% **2b** (green circles), and (e) slopes extracted from the SAXS profiles in Figures 3d and 4d in the range q = 0.4−0.5 nm^{-1} with respect to weight percent of **2**.

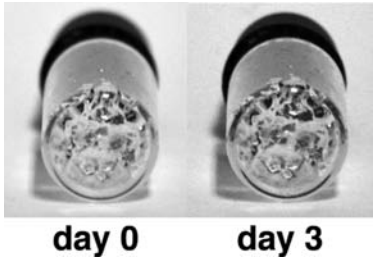

Figure 6. Self-healing experiment of a 5.0 wt% mixed hydrogel containing 2.3 wt% **1** and 2.7 wt% **2b**. (Left) Hydrogel crushed on day 0. (Right) Crushed hydrogel on day 3.

viscoelastic materials whose physical properties can be modulated over 2 orders of magnitude in elastic modulus, G', with a maximum at 1.1 wt% for **1** with **2b**, in frequency sweep experiments (Figure 5d).

Strain sweep experiments indicate that the gels become more brittle as the fraction of **1** decreases in the mixtures with **2a** and **2b** with a concomitant decrease in the yield stress. Mixtures of **1** with a surfactant molecule, sodium dodecyl sulfate, at the same total weight percentages as examined for **1** and **2b** did not yield any viscoelastic material. This result demonstrates that non-covalent complementarity between both building blocks **1** and **2b** is required to prepare the supramolecular material. SAXS measurements (Figure 5e,f) reveal structural changes in the properties of the mixed transient network further supporting the observed mechanical properties. A considerable difference in the slopes in the intermediate q range, between 0.4 and 0.5 nm^{-1}, of the scattering profiles marks the transition from a fluid-like to a gel-like state (Figure 5e). This transition is shifted to lower concentrations of **2b** when mixed with **1**. Modeling these profiles allows us to extract the mesh size of the network, which corresponds to roughly 2 nm (see Supporting Information). Moreover, inter-fibrillar interactions of **2b** are modified through decreasing their supramolecular polymer c^* upon mixing in **1** (Figure 5f), facilitating cross-linking by **2b** at low weight percentages to form stiff aqueous materials.

These mixed supramolecular materials composed primarily of molecule **2b** and a small amount of **1** surprisingly lack the self-healing character observed in numerous supramolecular polymer transient networks,[19,25,27−29] including those predominantly composed of **1**. These mixed materials were found to be visually non-self-healing (Figure 6) over the course of at least a month and lacked thermo-reversible character when mainly

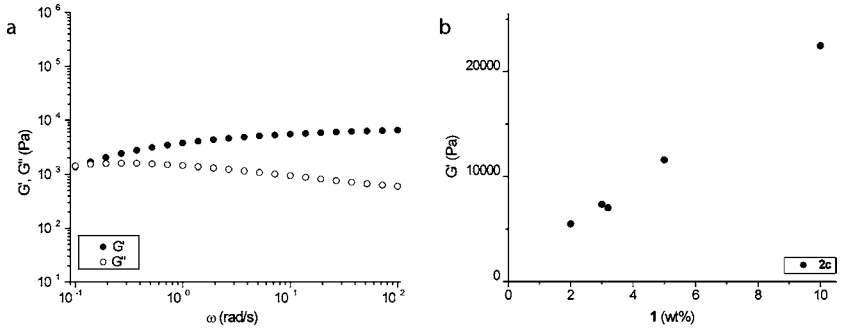

Figure 7. Oscillatory rheology measurements on mixed supramolecular materials composed of **1** and **2c**, after acidification (pH ~3). (a) Frequency sweep measurement (1% strain, 0.1−100 rad/s), representative profile of **1**, 3 wt%, and **2c**, 7 wt%. (b) Comparison of the plateau modulus as a function of increasing weight percentage of **1** with **2c** from the superposition of frequency sweep measurements.

dx.doi.org/10.1021/ja403745w | J. Am. Chem. Soc. 2013, 135, 11159−11164

composed of **2b**. A possible explanation for this less dynamic behavior of molecule **2b** can be extrapolated from its molecular structure; more specifically, the mass ratio of PEG to the hydrophobic linker. The PEG linker of molecule **1** (10 kDa) is 10 times greater in mass than molecule **2b** (780 Da). The mass difference of the hydrophilic moiety results in the increased dynamic character of **1**, where swelling of the supramolecular material is observed when submerged in excess water. Moreover, the shorter PEG chain length **2b** requires harsher conditions, i.e., high pH values, to achieve macroscopic dissolution. Additionally, these mixed materials were found to be practically non-eroding over a period of 7 days (see Supporting Information) upon exchanging the supernatant, thus highlighting the strong incorporation of both components **1** and **2b** into the 3D network. These results are in full accordance with oscillatory rheology data, where long relaxation times outside of the measuring range demonstrate the potential to kinetically trap or vitrify these mixed hierarchical assemblies.

Soft Dynamic Mixtures Composed of 1 and 2c. The strong synergistic effects found in the aqueous materials of **1** and **2a** or **2b** are based on the hypothesis of their distinct exchange rates in the transient supramolecular network. In order to validate this hypothesis, we synthesized **2c** containing the same PEG to hydrophobic fragment ratio as **1**. Monofunctional **2c** also forms fibrillar morphologies, but does not show any viscoelastic behavior even up to concentrations of 10 wt%. Hence, no interaction among the supramolecular fibrils occurs.

Gratifyingly, no rigid materials were obtained in the case of mixtures of **1** and **2c** as evidenced by the crossover of G' and G'' at long time scales (Figure 7a). The elastic modulus of mixtures of **1** and **2c** shows an almost linear dependence on the amount of cross-linker **1** added terminating at a maximum strength when composed exclusively of **1** (Figure 7b). Monofunctional **2c** seems to dilute the cross-links formed by **1**, indicating that a sufficient amount of cross-links are necessary to obtain gels when using larger hydrophilic blocks. These results show that mixtures based on **1** and **2c**, both having the same PEG to hydrophobic ratio, lack the synergistic effect observed for **1** to **2a** or **2b**, supporting the unique interaction of the combinations presented here.

CONCLUSION

Strong and stable hydrogels that outperform either component arise when small amounts of bifunctional UPy-PEG **1** are added to monofunctional UPy-PEGs **2a** or **2b**. Starting from components **1** and **2a,b** mixed in their solid state, we propose the following pathway in the construction of these hierarchically modulated mixed supramolecular materials with intermixed units (Figure 8). Dissolution of these structures under basic conditions proceeds via enolate formation on the UPy moiety, whereby electrostatic repulsion truncates and increases the dynamics of exchange of both fibrils. Of special note, neither monofunctional nor bifunctional fibrils are molecularly dissolved under these conditions, setting the stage for partial self-sorting of these molecules within the final assembly. Subsequent re-acidification converts the UPy group back to the keto/enol tautomers, effectively neutralizing and cross-linking these assemblies simultaneously. This step kinetically vitrifies the transient network resulting in a viscoelastic material of interacting fibrils based on strong non-covalent interactions. The ability to kinetically control the macroscopic properties of these metastable supramolecular materials in such a facile manner by structural changes at the mesoscale provides a wealth of subtly distinct mechanical properties as a function of supramolecular cross-linker added. We hypothesize the formation of such materials results from a large difference in the exchange rates of the supramolecular units in **1** and **2a,b**. In the co-assembly, where relatively fast exchange of **1** leads to self-healing, the slower exchange rate of **2b** vitrifies the stacks as observed by self-healing experiments and oscillatory rheology. This proposal is corroborated by the properties witnessed for the mixtures of **1** and **2c**, where the exchange rates are roughly equal due to similarity in ratio between the water-soluble PEG fragment and the hydrophobic fragment.

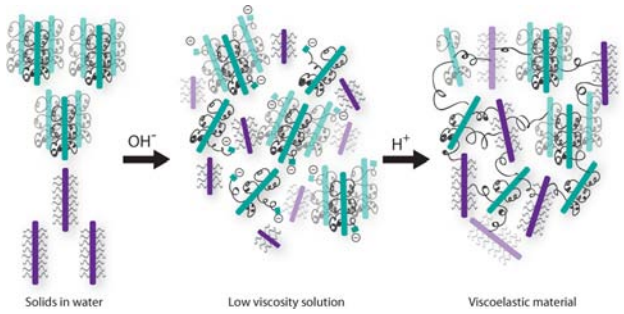

Figure 8. Scheme representing cross-linking of aggregates **2a,b** (purple) by **1** (green) to prepare the mixed supramolecular viscoelastic material. First, basic conditions (pH ∼12) permit dissolution of the fibers increasing their exchange, followed by acidic conditions (pH ∼3) locking in the hierarchical aggregate structure.

The behavior of this dual-fiber network is analogous to the interaction between actin fibers and their associated cross-linker proteins that modify the rheological properties of the cell. Understanding the range of physical properties attainable by this method provides a guide for the application of these aqueous supramolecular UPy-based materials in both chemistry and biology.

ASSOCIATED CONTENT

Supporting Information

Experimental details and characterization, including SAXS, AFM, SEM, rheology, and confocal microscopy of **2b** in solution at 0.01 and 5 wt%. This material is available free of charge via the Internet at http://pubs.acs.org.

AUTHOR INFORMATION

Corresponding Author

e.w.meijer@tue.nl

Notes

The authors declare no competing financial interest.

ACKNOWLEDGMENTS

We are supported by the Ministry of Education, Culture and Science (Gravity program 024.001.035), The Netherlands Organization for Scientific Research (NWO), and the European Research Council (FP7/2007-2013) ERC Grant Agreement. The small-angle X-ray experiments were performed at the Dutch-Belgian BM26B beamline of the European Synchrotron Radiation Facility, Grenoble, France, and the X12SA-cSAXS beamline at the Swiss Light Source of the Paul Scherrer Institut (PSI, Villigen, Switserland). We thank our local contacts Giuseppe Portale and Andreas Menzel for technical assistance with the SAXS experiments.

REFERENCES

(1) Pelletier, O.; Pokidysheva, E.; Hirst, L. S.; Bouxsein, N.; Li, Y.; Safinya, C. R. *Phys. Rev. Lett.* **2003**, *91*, 148102/1−148102/4.
(2) Lieleg, O.; Claessens, M. M. A. E.; Bausch, A. R. *Soft Matter* **2010**, *6*, 218−225.
(3) Zayed, J. M.; Nouvel, N.; Rauwald, U.; Scherman, O. A. *Chem. Soc. Rev.* **2010**, *39*, 2806−2816.
(4) Rybtchinski, B. *ACS Nano* **2011**, *5*, 6791−6818.
(5) Hartgerink, J. D.; Beniash, E.; Stupp, S. I. *Science* **2001**, *294*, 1684−1688.
(6) Besenius, P.; Portale, G.; Bomans, P. H. H.; Janssen, H. M.; Palmans, A. R. A.; Meijer, E. W. *Proc. Natl. Acad. Sci. U.S.A.* **2010**, *107*, 17888−17893.
(7) Obert, E.; Bellot, M.; Bouteiller, L.; Andrioletti, F.; Lehen-Ferrenbach, C.; Boué, F. *J. Am. Chem. Soc.* **2007**, *129*, 15601−15605.
(8) Sun, J.-Y.; Zhao, X.; Illeperuma, W. R. K.; Chaudhuri, O.; Oh, K. H.; Mooney, D. J.; Vlassak, J. J.; Suo, Z. *Nature* **2012**, *489*, 133−136.
(9) Steed, J. W. *Chem. Commun.* **2011**, *47*, 1379−1383.
(10) Van Bommel, K. J. C.; Van Der Pol, C.; Muizebelt, I.; Friggeri, A.; Heeres, A.; Meetsma, A.; Feringa, B. L.; Van Esch, J. *Angew. Chem., Int. Ed.* **2004**, *43*, 1663−1667.
(11) Rodríguez-Llansola, F.; Escuder, B.; Miravet, J. F. *J. Am. Chem. Soc.* **2009**, *131*, 11478−11484.
(12) Cui, H.; Webber, M. J.; Stupp, S. I. *Biopolymers* **2010**, *94*, 1−18.
(13) Schneider, J. P.; Pochan, D. J.; Ozbas, B.; Rajagopal, K.; Pakstis, L.; Kretsinger, J. *J. Am. Chem. Soc.* **2002**, *124*, 15030−15037.
(14) Jayawarna, V.; Ali, M.; Jowitt, T. A.; Miller, A. F.; Saiani, A.; Gough, J. E.; Ulijn, R. V. *Adv. Mater.* **2006**, *18*, 611−614.
(15) Zhang, Y.; Gu, H.; Yang, Z.; Xu, B. *J. Am. Chem. Soc.* **2003**, *125*, 13680−13681.
(16) Holmes, T. C.; de Lacalle, S.; Su, X.; Liu, G.; Rich, A.; Zhang, S. *Proc. Natl. Acad. Sci. U.S.A.* **2000**, *97*, 6728−6733.
(17) Gauba, V.; Hartgerink, J. D. *J. Am. Chem. Soc.* **2007**, *129*, 2683−2690.
(18) Tomatsu, I.; Hashidzume, A.; Harada, A. *Macromolecules* **2005**, *38*, 5223−5227.
(19) Buerkle, L. E.; Rowan, S. J. *Chem. Soc. Rev.* **2012**, *41*, 6089−6102.
(20) Hirst, A. R.; Smith, D. K. *Chem.—Eur. J.* **2005**, *11*, 5496−5508.
(21) Hirst, A. R.; Smith, D. K.; Feiters, M. C.; Geurts, H. P. M. *Langmuir* **2004**, *20*, 7070−7077.
(22) Das, R. K.; Kandanelli, R.; Linnanto, J.; Bose, K.; Maitra, U. *Langmuir* **2010**, *26*, 16141−16149.
(23) Smith, M. M.; Smith, D. K. *Soft Matter* **2011**, *7*, 4856−4860.
(24) Boekhoven, J.; Brizard, A. M.; Van Rijn, P.; Stuart, M. C. A.; Eelkema, R.; Van Esch, J. H. *Angew. Chem., Int. Ed.* **2011**, *50*, 12285−12289.
(25) Dankers, P. Y. W.; Hermans, T. M.; Baughman, T. W.; Kamikawa, Y.; Kieltyka, R. E.; Bastings, M. M. C.; Janssen, H. M.; Sommerdijk, N. A. J. M.; Larsen, A.; van Luyn, M. J. A.; Bosman, A. W.; Popa, E. R.; Fytas, G.; Meijer, E. W. *Adv. Mater.* **2012**, *24*, 2703−2709.
(26) Bastings, M. M. C.; Koudstaal, S.; Kieltyka, R. E.; Nakano, Y.; Pape, A. C. H.; Feyen, D. A. M.; van Slochteren, F. J.; Doevendans, P. A.; Sluijter, J. P. G.; Meijer, E. W.; Chamuleau, S. A. J.; Dankers, P. Y. W. *Adv. Healthcare Mater.* **2013**, DOI: 10.1002/adhm.201300076.
(27) Harada, A.; Kobayashi, R.; Takashima, Y.; Hashidzume, A.; Yamaguchi, H. *Nat. Chem.* **2011**, *3*, 34−37.
(28) Wang, Q.; Mynar, J. L.; Yoshida, M.; Lee, E.; Lee, M.; Okuro, K.; Kinbara, K.; Aida, T. *Nature* **2011**, *463*, 339−343.
(29) Yamaguchi, H.; Kobayashi, R.; Takashima, Y.; Hashidzume, A.; Harada, A. *Macromolecules* **2011**, *44*, 2395−2399.